Bax-derived membrane-active peptides act as potent and direct inducers of apoptosis in cancer cells.

Juan Garcia Valero, Lucie Sancey, Jérôme Kucharczak, Yannis Guillemin, Diana Gimenez, Julien Prudent, Germain Gillet, Jesús Salgado, Jean-Luc Coll, Abdel Aouacheria

Bax-derived membrane-active peptides act as potent and direct inducers of apoptosis in cancer cells

Juan Garcia Valero [1] **, Lucie Sancey** [2] **, Jérôme Kucharczak** [1] **, Yannis Guillemin** [1] **, Diana Gimenez** [3] **, Julien Prudent** [1] **, Germain Gillet** [1] **, Jesús Salgado** [3 4] **, Jean-Luc Coll** [2] **, Abdel Aouacheria** [1 *]

[1] *IBCP, Institut de biologie et chimie des protéines* [*Lyon*] *CNRS : UMR5086 , Université Claude Bernard - Lyon I , 7 Passage du Vercors 69367 LYON CEDEX 07,FR*

[2] *Institut d'oncologie/développement Albert Bonniot de Grenoble INSERM : U823 , CHU Grenoble , EFS , Université Joseph Fourier - Grenoble I , Institut Albert Bonniot, BP170, 38042 Grenoble Cedex 9,FR*

[3] *Instituto de Ciencia Molecular Universidad de Valencia , Polígono La Coma, s/n, 46980 Paterna, Valencia,ES*

[4] *Departamento de Bioquímica y Biología Molecular Universidad de Valencia , C/ Doctor Moliner, 50, 46100 Burjassot, Valencia,ES*

* Correspondence should be addressed to: Abdel Aouacheria <a.aouacheria@ibcp.fr >

Abstract
SUMMARY

Although many cancer cells are primed for apoptosis, they usually develop resistance to cell death at multiple levels. Permeabilization of the outer mitochondrial membrane, which is mediated by proapoptotic Bcl-2 family members like Bax, is considered as a point-of-no-return for initiating apoptotic cell death. This crucial role has placed Bcl-2 family proteins as recurrent targets for anticancer drug development. Here, we propose and demonstrate a new concept based on using minimal active version of Bax to induce cell death independently of endogenous Bcl-2 proteins. We show that membrane-active segments of Bax can directly induce the release of mitochondria-residing apoptogenic factors and commit tumor cells promptly and irreversibly to caspase-dependent apoptosis. On this basis, we designed a peptide encompassing part of the Bax pore-forming domain, able to target mitochondria, induce cytochrome c release and trigger caspase-dependent apoptosis. Moreover, this Bax-derived poropeptide produced effective tumor regression after peritumoral injection in a nude mouse xenograft model. Thus, peptides derived from proteins evolutionary functionalized to form pores in the mitochondrial outer membrane represent novel templates for anticancer agents.

MESH Keywords Animals ; Antineoplastic Agents ; chemistry ; metabolism ; pharmacology ; Apoptosis ; drug effects ; Cell Line, Tumor ; Cytochromes c ; metabolism ; Humans ; Mice ; Mitochondria ; drug effects ; metabolism ; Neoplasms ; drug therapy ; physiopathology ; Peptides ; chemistry ; genetics ; metabolism ; pharmacology ; Protein Structure, Tertiary ; bcl-2-Associated X Protein ; chemistry ; genetics ; metabolism ; pharmacology

Author Keywords apoptosis ; Bcl-2 family ; proapoptotic Bax ; mitochondria ; pore-forming peptides ; anticancer agent ; antivascular therapy

INTRODUCTION

The integrity of the mitochondrial outer membrane (MOM) serves as a switch between cell survival and cell death by apoptosis. The Bcl-2 family of proteins are critical arbiters in this process due to their ability to either promote or inhibit MOM permeabilization (Aouacheria et al., 2007 ; Youle and Strasser, 2008). Pro-apoptotic members (e.g. Bax, Bak, BH3-only proteins) promote cytochrome c release from mitochondria, leading to the activation of proteases termed caspases that mediate cell demise. Conversely, anti-apoptotic members such as Bcl-2 or Bcl-xL decrease cell death susceptibility by neutralizing Bax/Bak or BH3-only proteins.

Over-expression of pro-survival proteins occurs in many human tumors, and can contribute not only to disease development and progression but also to clinical drug resistance (Adams and Cory, 2007). Anti-apoptotic Bcl-2 family members therefore represent prime targets for the development of modern anticancer drugs that have the potential to restore apoptosis and reverse resistance to chemotherapy. Efforts to inhibit the anti-death Bcl-2 family members have focused on the development of cell-permeable peptides or small-molecule inhibitor drugs, designed to mimic the BH3 domain of Bcl-2 family death members (Yip and Reed, 2008). A number of such BH3 mimics (e.g. ABT-737) (Oltersdorf et al., 2005), which inactivate Bcl-2-like proteins by binding to their BH3-binding groove, have now entered clinical trials and provide real opportunities for improving the efficacy of cancer treatment. Recently, another strategy has been described that converts pro-survival Bcl-2 molecules into pro-apoptotic proteins with the potential to kill cancer cells. In this new approach, a short peptide derived from the orphan nuclear receptor Nur77 was shown to bind to the N-terminal regulatory region of Bcl-2, altering its structure to expose its BH3 domain, which then becomes free to activate Bax/Bak (Kolluri et al., 2008). However, one major common limitation of these two latter strategies is that they depend on endogenous levels of anti-apoptotic Bcl-2 proteins in cancer cells. Moreover, these strategies are expected to be less effective in inducing apoptosis of tumor cells with mutated or deficient Bax or Bak (Jansson and Sun, 2002 ; Ouyang et al., 1998 ; Zong et al., 2001).

While apoptosis signaling pathways are often compromised during malignant transformation, mitochondria-resided apoptogenic factors are still present in cancer cells and it is an exciting challenge to develop peptides or peptidomimetics capable of inducing their

release. Such molecules would have the capacity to promote MOM permeabilization directly, and thus to overcome cancer cell resistance towards apoptosis induction. Furthermore, molecules that function at the membrane level are less likely to encounter resistance than drugs based on classical lock-and-key binding specificity. Following these ideas, it has been shown in several studies that, upon cell internalization, antimicrobial peptides (e.g. $(KLAKLAK)_2$) can induce cell death in a variety of cell types (Chen et al., 2001 ; Ellerby et al., 1999 ; Foillard et al., 2008 ; Foillard et al., 2009 ; Law et al., 2006 ; Mai et al., 2001 ; Marks et al., 2005 ; Rege et al., 2007). However, the mechanisms of cell killing exerted by these antibiotic peptides are unclear, as they appear to include both necrosis, secondary to plasma membrane disruption (Papo et al., 2006), and apoptosis induced either by upregulation of death effectors (Chen et al., 2001) or by mitochondrial membrane permeabilization (Ellerby et al., 1999 ; Law et al., 2006 ; Mai et al., 2001 ; Marks et al., 2005 ; Rege et al., 2007). Noteworthy, the cationic peptide $(KLAKLAK)_2$ has been reported to have very low potency (Borgne-Sanchez et al., 2007 ; Ellerby et al., 1999), which precludes its use as an effective anticancer drug.

In this context, it is an important goal to identify novel pro-apoptotic sequences, acting directly at the level of mitochondrial permeability, which can be exploited to engineer potent anticancer molecules. Among the potential candidates are membranolytic peptides derived from proapoptotic Bcl-2 family proteins such as Bax. This 23-kD protein contains a number of structurally defined membrane-interacting regions (Suzuki et al., 2000), some of them (α1, α9, α5, α6 and a central α5α6-hairpin motif) with a presumed membrane-targeting function (Annis et al., 2005 ; Cartron et al., 2005 ; Garcia-Saez et al., 2004 ; Heimlich et al., 2004). It has been previously shown that peptides corresponding to the first and/or to the second helix of the putative pore-forming domain of Bax (α5-α6 hairpin) can reproduce, at least in part, the poration activity displayed by the full-length parent protein (Garcia-Saez et al., 2005 ; Garcia-Saez et al., 2006 ; Guillemin et al.). Hence, helices α5-α6 of Bax carry by themselves minimal structural information and physicochemical properties to insert into model lipid membranes and form pores. The pores appear to be of the mixed lipidic-peptidic type (Garcia-Saez et al., 2007 ; Qian et al., 2008), similar to those of membrane-active, amphipathic peptide antibiotics (Fuertes et al., 2010). Here, we report that the two central helices of Bax individually are sufficient to target GFP to mitochondria and induce caspase-dependent cell death. Moreover, we demonstrate that a peptide designed from helix 5 can induce directly the release of mitochondrial cytochrome c, thereby acting as a potent apoptosis activator. This peptide, named poropeptide-Bax[106-134], was more efficient for both mitochondrial targeting and apoptosis induction than $(KLAKLAK)_2$, a *de novo* synthetic peptide. Finally, we report a clear anticancer effect of poropeptide-Bax[106-134] after peritumoral administration in tumor-bearing mice. Our data establish the feasibility of using short peptides derived from mitochondrial outer membrane-porating proteins as a basis for designing novel anticancer agents, which may be directly applied to some solid tumors or homed to the tumor microenvironment through the use of specific vectors.

RESULTS

Bax-α5/α6-containing constructs induce caspase-dependent apoptosis in transfected cells

In a search for peptide sequences capable of targeting and disrupting the MOM, recombinant constructs encoding the GFP open reading frame fused to the N-terminus of various membrane-active fragments of Bax (α1, α9, α5, α6, α5α6 and α5-α9) were prepared (see definition of fragments and schemes of constructs in Fig. 1A). Western blot analysis confirmed the correct size of the fusion proteins (Fig. 1B , upper panel). The different constructs were transfected into human HT1080 cells and cell death was measured after 24h. As a measure of cell viability, GFP-positive cells were analyzed by Annexin V staining (Fig. 1C) or scored for nuclear apoptosis (as assessed by morphology) or necrosis (by staining with propidium iodide) (Fig. S1 , top and middle). GFP alone, GFP-Bax and GFP–Bax-α1 had no cytotoxic effect. The other constructs were all able to induce predominantly apoptotic cell death, with maximum activity observed after transfection with GFP–Bax-α5α6, GFP–Bax-α5 and GFP-Bax-α6, and intermediate levels for GFP–Bax-α5-α9 and GFP–Bax-α9. Furthermore, fusion proteins including the α5 and/or α6 helices of Bax elicited caspase-3 and PARP cleavage, as evidenced by western blot (Fig. 1B , bottom and middle panels, respectively). Consistently, treatment with 100μM zVAD.fmk, a cell-permeable caspase inhibitor, was effective in reducing cell death induced by the toxic GFP fusion proteins (Fig. S1 , middle), indicating that cell death is caspase-dependent. Importantly, the pro-apoptotic effects of the Bax-derived constructs were not exerted through Bax and Bak, because Bax/Bak double knockout MEFs (MEF DKO) were as sensitive as wild-type MEFs to Bax-α5 expression (Fig. S1 , bottom), while being resistant to staurosporine treatment (Fig. 1D).

Fusions including Bax-α5/α6 localize to mitochondria and alter the organelle physiology

The subcellular localization of all assayed GFP-tagged Bax fragments was subsequently evaluated by confocal fluorescence microscopy. Expression of the fusion proteins yielded abundant and intense GFP fluorescence in transfected MEF-DKO cells (Fig. 2). GFP alone showed a diffuse localization. Similarly, GFP–Bax and GFP–Bax-α1 distributed evenly between the nuclear and cytoplasmic compartments in transfected cells. In contrast, confocal imaging revealed that GFP–Bax-α5, GFP–Bax-α6, GFP–Bax-α5α6, GFP–Bax-α5-α9 and GFP–Bax-α9 exhibited a clustered staining, reminiscent of intracellular membranes. The simultaneous use of a mitochondrion-specific red marker (mitoDsRed) indicated that this punctuated staining colocalized with mitochondria. This was confirmed

by immunostaining of GFP-Bax-α5-transfected cells using anti-mitoHsp70, which shows that a large portion of the fusion protein is indeed specifically associated with mitochondria (Fig. 2 , bottom). Of note, GFP-Bax-α5 was also found to be more efficient for mitochondrial targeting than a fusion containing the sequence of the designed proapoptotic peptide $(KLAKLAK)_2$ (Fig. 2).

Mitochondria dependent apoptosis typically affects the homeostasis of the organelle, which can be investigated by tracing changes of the mitochondrial membrane potential ΔΨm. Thus, using the membrane-potential sensitive dye Mitotracker Red CMXRos, we measured ΔΨm in cells expressing either MOM-targeting sequences (GFP–Bax-α5, GFP–Bax-α6, GFP–Bax-α5α6, GFP–Bax-α5-α9 and GFP–Bax-α9) or non-targeting sequences (GFP and GFP–Bax-α1). Examination of individual cells showed that those having strong expression of the cytotoxic, MOM-targeting GFP-tagged fusions exhibited a concomitant decrease of Mitotracker Red staining (Fig. 3 and Fig. S2 , top panel), meaning a loss of the mitochondrial membrane permeability. Analysis of ΔΨm changes by FACS yielded comparable results (Fig. S2 , middle and bottom), with values correlating with the apoptotic activity.

From the experiments described so far, we can conclude that the sequences from the central hairpin of Bax as well as the Bax TM domain (α9) contain the necessary information to target the GFP protein specifically to the mitochondrial membranes. However, the Bax-α5- or Bax-α6-containing chimeras distinguish themselves from the GFP-Bax-α9 fusion by being markedly more active for inducing depolarization of the mitochondrial membrane and caspase-dependent apoptosis. Both Bax-α5 and Bax-α6, either in the Bax protein (Suzuki et al., 2000) or as individual peptides bound to membranes (Garcia-Saez et al., 2005 ; Garcia-Saez et al., 2006) form amphipathic α-helices. Additionally, they have a similar ratio of hydrophilic to hydrophobic residues (31% and 33%, respectively). However, the expected net charge of these fragments is very different at neutral pH, namely: +4 for Bax-α5 and −1 for Bax-α6, indicating that Bax-α5 is a better candidate for binding and disruption of the mitochondrial outer membrane, rich in negatively charged phospholipids. This is indeed suggested by the higher membrane depolarization observed for chimeras containing Bax-α5. For this reason, in the following stages of our work we focus on the Bax-α5 active fragment, as a prototype for proof-of-concept evaluation.

A synthetic peptide corresponding to Bax residues 106-134 exhibits potent mitochondrial-poration activity

Based on the above findings, we tested whether a synthetic peptide with the sequence of helix α5 from Bax, residues Asn^{106} to Arg^{134} (Fig. S3 , panel A, inset), can induce cytochrome c release from freshly prepared mitochondria (isolated from SK-MEL-28 metastatic human melanoma cells). A 5-min exposure to 10 μM of the Bax[106-134] peptide was sufficient to cause significant release of mitochondrial cytochrome c, and a concentration of 25 μM completely depleted all mitochondrial cytochrome c after the same incubation time (Fig. S3A , panel A, top). For comparison, we also assayed a peptide corresponding to the BH3 domain of Bax (helix-α2), which was found to have no effect (Fig. S3 , panel A, middle). Importantly, unlike the Bax[106-134] peptide, the synthetic $(KLAKLAK)_2$ peptide was unable to release cytochrome c from isolated mitochondria (Fig. S3 , panel A, bottom). These results demonstrate that a synthetic, native (non-optimized) peptide encompassing the helix-α5 of Bax can on its own disrupt mitochondrial membrane permeability and induce release of cytochrome c. Such an activity is specific of this Bax-derived sequence, as it is not observed at comparable conditions by using another helical fragment of Bax with no reported poration activity (helix-α2, i.e. Bax-BH3.). This peptide derived from the BH3 domain of Bax displayed only a weak activity, starting at 25μM after 30–60 min of peptide exposure, using human embryonic kidney HEK293T cells. Additionally, a similar activity is also not observed for the antimicrobial peptide $(KLAKLAK)_2$, showing that the sequence of the Bax[106-134] active fragment has been optimized during natural evolution for this particular function. Further support for the mitochondrial disruption capacity of Bax[106-134] was obtained by measuring peptide-induced swelling (SD50 = 3.98 ± 0.57 μM) and ΔΨm dissipation (DD50 = 1.68 ± 0.39 μM) (Fig. S3 , panel B) on liver mitochondria, two characteristics indicative of mitochondrial membrane permeabilization. These results illustrate the particularly strong capacity of the Bax[106-134] peptide to trigger mitochondrial membrane perforation. Moreover, they provide rationale for the development of MOM-permeabilizing peptides inspired by helix α5 of Bax, which may then be used to induce apoptosis in cancer cells.

Bax[106-134] fused to an octarginine cell penetrating motif induces caspase-dependent cell death

Next, we set out to investigate the effect of the Bax[106-134] peptide in cultured cells. One requirement for these experiments is the efficient delivery of the peptide, which should first cross the cell membrane to reach mitochondria and induce MOM permeabilization. In order to drive translocation across the plasma membrane, we used a modified version of the peptide with a poly-Arg sequence at the N-terminus (eight residues) connected to the natural sequence through a Gly linker (R8-Bax[106-134]). In addition, the peptide was derivatized with a fluorescent FITC label at its N-terminus to allow easy detection. A control peptide with similar design but with a scrambled version of the Bax[106-134] natural sequence was also synthesized (R8-Bax[Scr]). This scrambled version will not be amphipathic in its expected membrane-bound α–helix conformation. Dose-response analyses were undertaken, incubating HeLa cells with the peptides at different concentrations and different exposure times, monitoring cellular uptake and cell viability. Fluorescence microscopy revealed uptake of both peptides, with strong green fluorescence observed in the cytoplasm as early as 1h after exogenous administration at a concentration of 10μM (Fig. 4A). However, although R8-Bax[Scr] penetrated efficiently into HeLa cells, this peptide did not produced any significant cellular toxicity, as assessed by lactate dehydrogenase (LDH) release (Fig. 4B). In contrast, R8-Bax[106-134] induced cell death in a dose- and time-dependent manner with LC_{50} ~ 15μM at 24h. As depicted in Fig. 4C , the R8-Bax[106-134]

-induced LDH release was significantly diminished by incubation with zVAD.fmk, suggesting that cell death follows a caspase-dependent pathway. This observation was supported by Hoechst/propidium iodide double staining analysis (Fig. 4D), which confirmed that cell death was due to apoptosis. Moreover, we found that R8-Bax[106-134] induced similar levels of toxicity (analyzed by flow cytometry using Annexin-V binding) in Bax/Bak-deficient mouse embryonic fibroblasts (MEF DKO) and wild-type cells (MEF) (Fig. 5), whereas the corresponding scrambled peptide R8-Bax[Scr] had no effect. Treatment with the caspase inhibitor zVAD.fmk blunted R8-Bax[106-134] -induced cytotoxicity in both cell types. These results further confirm that the cell death observed is independent of both BAX and BAK (consistent with our previous data using isolated mitochondria, (Guillemin et al.)) and is occurring via caspase-dependent apoptosis. The R8-Bax[Scr] version can also be considered as a control to show that the cell death induced by R8-Bax[106-134] is not linked to the presence of the R8 sequence. We formally demonstrated that cytotoxicity was R8-independent by microinjecting into zebrafish eggs and human melanoma SK-MEL-28 cells a naked Bax[106-134] peptide (not fused to any protein transduction domain) or an octa-arginine peptide (R8). Results showed that the apoptotic activity of R8-Bax[106-134] was specific of the natural Bax-α5 sequence and not of the membrane translocating poly-Arg motif (Fig. S4 and Fig. S5).

Cytotoxic Bax[106-134] injected peritumorally shows antitumor activity in vivo

Fluorescence data obtained using a non-invasive live animal imaging technology indicated that, upon peritumoral administration, a Cy5-labeled Bax[106-134] peptide was mainly taken up by the tumor tissue, which exhibited strong Cy5 fluorescence intensity even 24h after injection (Fig. S6 , panel A). Moreover, *ex vivo* fluorescence images of excised tumor tissues indicated minor accumulation to adjacent normal tissue (Fig. S6 , panel B). These fluorescence data suggested that the Cy5-labeled peptide had a sustained localization within the tumor micro-environment following peritumoral injection, which prompted us to investigate the anti-tumor activity of Bax[106-134] using this administration mode. To test the antitumor efficacy, the R8-Bax[106-134] version, or control samples (the scrambled R8-Bax[Scr] peptide or buffer alone), were injected peritumorally 5 times a week for 2 weeks in mammary adenocarcinoma (TS/A-pc) tumor-bearing athymic nude mice. As shown in Fig. 6 , after 2 weeks of peritumoral administration, the tumor volume was sharply reduced in the group treated with R8-Bax[106-134], compared to the control groups. There was a statistically significant decrease in tumor size, tumor doubling time and growth. Moreover, tumor size reduction correlated with an increase in caspase-3 positive cells in tumor tissue extracts indicating cell death (Fig. 6 , *inset*).

DISCUSSION

Aside from the intrinsic biotechnological potential of biodiversity, properties of molecules found in Nature can be mimicked or extended to produce novel bioactive substances. In this respect, the BH3-mimetic strategy represents a relevant example of the translation of molecular discoveries into potential clinical applications (Yip and Reed, 2008). Membrane-active peptides acting on the MOM (i.e. able to induce cytochrome c release and apoptosis) represent yet another type of promising, but so far unexploited, candidates in the cancer research field (Chen et al., 2001 ; Ellerby et al., 1999 ; Foillard et al., 2008 ; Law et al., 2006 ; Mai et al., 2001 ; Marks et al., 2005 ; Rege et al., 2007). Such a strategy has some parallel with the development of antibiotics from natural antimicrobial peptides (Marr et al., 2006), and in fact the use of these latter systems as anticancer drugs has already been proposed (Ellerby et al., 1999 ; Mader and Hoskin, 2006 ; Papo and Shai, 2005). As a singular advantage, and unlike the pro-apoptotic BH3-derived peptides or BH3-like compounds, mitochondrial membrane disrupting peptides will be active in cancer cells that do not express Bcl-2-like proteins, or in neo-angiogenic endothelial cells irrespective of the Bcl-2 family status. Additionally, compared to other membranolytic peptides of different sources, active fragments designed from pore forming Bcl-2 proteins can be considered to be naturally optimized by evolution to act on mitochondrial membranes (Guillemin et al.). Here, we have shown that a peptide (Bax[106-134]) derived from the pore-forming domain of pro-apoptotic Bax can cause mitochondrial damage and caspase-dependent apoptosis. This peptide appears to carry sufficient structural information to insert into the MOM, causing ΔΨm loss, membrane disruption and cytochrome c release. Moreover, it produced (when fused to a polyarginine transduction motif) potent anticancer activity after peritumoral injection in tumor-bearing mice presumably by inducing tumor cell apoptosis.

The molecular mechanism of pore formation and the structural properties of different peptide versions encompassing the sequence of helix α5 from Bax (which were very similar to Bax[106-134]) have been studied in several recent papers (Garcia-Saez et al., 2007 ; Garcia-Saez et al., 2005 ; Garcia-Saez et al., 2006 ; Guillemin et al.; Qian et al., 2008). These different versions of the α5 fragment of Bax exhibited strong α-helical propensity in model lipid membranes and were shown to form lipidic pores of toroidal structure (Garcia-Saez et al., 2005 ; Qian et al., 2008). A similar mechanism of pore formation has been proposed for cationic α-helical antimicrobial peptides like magainin (Ludtke et al., 1996). Although Bax has also been proposed to form pores of the proteo-lipidic toroidal type (Terrones et al., 2004), its mechanism of action is still largely unknown. A major difference between the activity of complete Bax, compared to that of Bax fragments, towards mitochondrial membranes is the existence of upstream (yet unclear) regulatory events, leading to Bax activation via structural reorganization and membrane binding. Additionally, in the active membrane-bound state, the Bax protein surely forms a larger and more complex oligomer and pore than Bax-derived peptides. Nevertheless, our results are consistent with the main findings reported in the literature for Bax action. First, the GFP fusion to complete Bax shows no specific localization to mitochondria (Fig. 2), weak disrupting activity towards this organelle (Fig. 3 and S2) and weak apoptosis induction (Fig. 1 and S1). This result is in accordance with

the notion that monomeric Bax has to be activated by tBid previous to its targeting, oligomerization and poration of the MOM (Billen et al., 2008 ; Lovell et al., 2008 ; Terrones et al., 2004). In contrast, Bax fragments display a clearly different behaviour. Fusions of GFP with Bax fragments containing α5, α6 and/or α9, either alone or in the α5-α6 or α5-α9 constructions, all localize specifically and intrinsically to mitochondria (Fig. 2). In contrast, the fusions containing only the α5 and α6 fragments as well as the α5-α6 hairpin miniature exhibit a high mitochondria-disrupting activity (Fig. 3 and S2), which, in turn, correlates with strong cell death induction (Fig. 1 and S1). These latter and most remarkable observations are consistent with the existence in Bax of several independent mitochondrial targeting sequences, located in helices α5, α6 and α9 (George et al., 2007 ; George et al.; Schinzel et al., 2004 ; Valentijn et al., 2008). Thus, our results show that the naked versions of these fragments have a natural tendency for specific binding to the MOM, and in the cases of α5 and α6 for high membrane poration activity, with no need for complex structural reorganization, as they are intrinsically active. Within the context of larger domains, intra- and inter-molecular interactions between different helices of Bax (George et al., 2007 ; George et al.; Suzuki et al., 2000) may impair their interaction with the membrane. This phenomenon, which is at the origin of the regulation of the complete Bax protein, might also be among the reasons why the GFP-Baxα5-α9 construct was not as potent as Baxα5, -α6 and -α5α6 in causing cell death (Fig. 1 and S1).

In conclusion, although Bax-derived fragments can obviously not mimic the elaborate behaviour of the full length protein, considering fundamental aspects of their membrane activity, these peptides represent in practice minimal versions of Bax, evolutionary-designed to target, bind and porate mitochondria. Thus, Bax[106-134] shows a specificity and efficacy for MOM disruption clearly overcoming that of the cationic peptide $(KLAKLAK)_2$, in agreement with the low potency previously reported for this molecule (Borgne-Sanchez et al., 2007 ; Ellerby et al., 1999). Additionally, the lack of regulatory capacity in minimal peptide versions with respect to full-length Bax renders these molecules intrinsically and autonomously active, which may be used advantageously as a basis for antitumor therapy. Thus, we propose to exploit membrane-active segments from natural Bcl-2-like templates (such as helices α5/6 of Bax) to develop a new generation of mitochondria-targeted cytotoxic agents (named poropeptides). To be applicable in cancer therapy, poropeptides should eliminate tumor cells without being harmful to normal cells. Indeed, although such biologically active peptides can be developed into drugs, design of suitable delivery systems for site-specific targeting to tumors remains the most challenging task. Future work will therefore focus on endowing therapeutic poropeptides with the ability to reach tumor cells and leave normal cells unharmed.

MATERIAL AND METHODS

Peptides

Bax[106-134], Bax-BH3, FITC-R8-Bax[106-134], FITC-R8-Bax[Scr] and R8 peptides were purchased from GeneCust EUROPE at a 2 or 5 mg scale and purified to >95% by HPLC. R8-Bax[106-134] and R8-Bax[Scr] were prepared by solid-phase synthesis as reported (Garcia-Saez et al., 2005) in an Applied Biosystems ABI 433A Peptide synthesizer (Foster City, CA, USA) using Fmoc chemistry and Tentagel S-RAM resin (Rapp Polymere, Tübingen, Germany; 0.24 mEq/g substitution) as a solid support. Peptides were purified using a C18 semi-preparative reversed-phase column (Merck, Darmstadt, Germany) by HPLC, to a >95% purity, and their identity was confirmed by Mass Spectrometry. Peptide concentrations were determined from UV spectra using a Jasco spectrophotometer (Jasco, Tokyo, Japan). The Cyanine5-Bax[106-134] peptide was synthesized using solid-phase peptide synthesis (SPPS), purified by HPLC and characterized by ESMS at the chemistry platform NanoBio campus (Grenoble, France). R8 (arginine-8) peptides had an amide group at their C-terminus. The amino acid sequences of the peptides are shown in Table I.

Antibodies

Primary antibodies were as follows: mouse monoclonal Anti-mitochondrial-HSP70 (Abcam), anti-GFP mouse monoclonal antibody (Roche), anti-cleaved caspase-3 rabbit polyclonal antibody (Cell Signaling Technology), anti-cleaved PARP (Abcam), anti-α-tubulin antibody (Santa Cruz Biotechnologies) and anti-cytochrome c antibody. HRP-conjugated goat anti-mouse and goat anti-rabbit secondary antibodies (Roche) were used as secondary antibodies. Western Blot analysis was performed according to standard procedures.

Cell culture

SK-MEL-28 human melanoma cells and HeLa cells were cultured at 37°C and 5% CO_2 in MEM supplemented with 10% FBS, 1% penicillin/streptomycin and 1% of non-essential amino acids. HT1080 cells, HEK293T cells, MEF and MEF-DKO mouse embryonic fibroblasts cells were cultured in DMEM supplemented with 10% FBS and 1% Penicillin/Streptomycin. For transient transfection, cells were plated at a density of 10^5 cells per 35mm plate) and allowed to grow for 24h before transfection with plasmids using the Lipofectamine 2000 (Invitrogen) according to the manufacturer s recommendation. For each transfection 3 μg plasmid DNA was used. Caspase inhibitor zVAD.fmk was purchased from Bachem. TS/A-pc mice mammary carcinoma cells were cultured in RPMI 1640 supplemented with 1% glutamine, 10% FBS, 50 units/ml penicillin, and 50 μg/ml streptomycin at 37°C in a humidified 95% air/5% CO_2 atmosphere. These cells are integrin αvβ3-positive (Klepfish et al., 1993 ; Sancey et al., 2007).

Molecular cloning

The oligonucleotides (Sigma-Proligo) that were used to prepare the different constructions are indicated in Table S1 . All the constructions were subcloned into pGEM-T Easy (Promega) and then subsequently subcloned into XhoI and KpnI sites of pEGFP-C1. The sequence of all constructs was verified by automated sequencing (GEXbyWeb).

Measurement of cell death and viability

Hoechst/PI labeling of cells to detect apoptotic and necrotic cell death were performed as described previously (Dive et al., 1992). Hoechst 33342 and PI were from Molecular Probes (Invitrogen). LDH cytotoxicity assay was performed according to the manufacturer's protocol (LDH Cytotoxicity Assay Kit II, Biovision Research Products, CA); the colorimetric assay quantifies LDH activity released from the cytosol of damaged cells into the supernatant and thus serves to quantify cell death. Cytotoxicity assays were performed in triplicates in each of two or three independent experiments. Cell death was quantified by Annexin-V-Cy3 (BioVision Inc.) staining according to manufacturer's protocols, followed by flow cytometric analysis using a FACScan (Becton Dickinson). Data were processed using CellQuest Pro (version 4.0) software.

Mitochondrial assays

In vitro assessment of mitochondrial parameters (swelling and ΔΨm loss) was performed on liver mitochondria as previously described (Jacotot et al., 2006). Mitochondrial membrane potential was measured using the fluorescent dye Mito-Tracker Red (Molecular Probes), which emits fluorescence in cells with an intact ΔΨm. Transfected cells were incubated with Mito-Tracker Red (50 nM for 2h min at 37 °C). Cells were observed under a fluorescence microscope and the percentage of green cells that were Mito-Tracker positive was determined (~100 cells in each experiment). For flow cytometry analysis, HT1080 cells were washed twice with serum-free medium and then resuspended in PBS. Flow cytometric analysis was performed using a LSR II (Becton Dickinson) and data were processed using FACSDiva (version 6.1.2) software.

Confocal microscopy analysis

Cells were fixed in 4% paraformaldehyde, permeabilized in 0.1% Triton X-100 for 3 minutes, and treated with TO-PRO-3 iodide (final 2μM, Molecular Probes) before mounting in a drop of anti-bleaching medium. Confocal analysis was performed on a Zeiss confocal microscope (LSM510) (LePecq, France) with a plan apochromat 63 × 1.4 oil immersion objective. Images were collected under identical non-saturated conditions after multiple scans (~ 8 sections per cell).

***In vivo* experiments**

All the animal experiments were performed in agreement with the EEC guidelines and the “Principles of laboratory animal care” (NIH publication 14N°86-23 revised 1985). The experimental protocol was submitted to ethical evaluation and the experiment received the accreditation number #323. The investigator possesses the authorization number #38-09-22 (Sancey L.)

Tumor regression assays

Mouse mammary TS/A-pc cells were harvested from culture, and 10^6 cells in sterile PBS were injected subcutaneously into the flank of thirty female Balb/c mice. Three days after injection, mice were randomized into three experimental groups (9 mice/group). Group 1 (control mice) received vehicle (PBS), group 2 received Bax[106-134], and group 3 received Bax-Scr.

One hundred μg peptide/mouse (100 μl/mouse) was administered peritumorally, 5 times a week for 2 weeks. Tumor growth was assessed by measuring tumor size in two dimensions using a Vernier caliper each day after tumor size reaches 10 mm^3 or larger (from day 10). Tumor volume was calculated as follows: $(\pi/6) \times a \times b^2$, where a and b are the largest and smallest diameters, respectively (Kjonniksen et al., 1989 ; Olea et al., 1992). Results are expressed as mean ± S.E.M. None of the mice had developed necrotic tumors or tumors ≥ 1.5 cm in diameter. On day 14, all mice were sacrificed to prevent lung metastasis, especially in groups 1 and 3. The tumor doubling time (TDT) was calculated as $(Td'-Td)\ln 2/(\ln(Vd'-Vd))$, where T is time at days d and d′ and V is the corresponding tumor volume.

Statistical analysis

For the *in vivo* studies, results were analyzed by *t* -test for unmatched groups (Statview software, SAS Institute, Inc.): *p* values < 0.05 were considered statistically significant.

Acknowledgements:

We wish to thank Julien Thibaut, Agnès Cibiel, Clara Locher, Jonathan Lopez and Sonia Schott for help during the initial stages of this work, Gustavo Fuertes (Universidad de Valencia, España) and Eric Diesis (IBCP) for the provision of peptides, Aurélie Cornut for guidance in cloning, Annie Borgne-Sanchez at Mitologics, Marie-Hélène Ratinaud and Nathalie Bonnefoy-Bérard for discussion. The MitoRed plasmid was a kind gift from Dr. Dong. JGV is recipient of doctoral fellowship from La Région Rhône-Alpes. LS is granted by ANR PNANO. We are

indebted to Jean Paufique, Brigitte Closs, Sylvie Bordes and Sandrine Magnetto for their constant support and for their continuous interest in this work. This work was supported by grants from the Silab-Jean Paufique Corporate Foundation (France), La Ligue Contre le Cancer (Comités de la Drôme et du Rhône), the Spanish MEC (BFU2007-67097) and a collaborative French/Spanish project (EGIDE PHC PICASSO 17092SM; MEC, HF2007-0090).

Footnotes:

CONFLICT OF INTEREST The authors declare that they have no conflict of interest.

References:

- Adams JM , Cory S . 2007 ; The Bcl-2 apoptotic switch in cancer development and therapy . Oncogene . 26 : 1324 - 37
- Annis MG , Soucie EL , Dlugosz PJ , Cruz-Aguado JA , Penn LZ , Leber B , Andrews DW . 2005 ; Bax forms multispanning monomers that oligomerize to permeabilize membranes during apoptosis . Embo J . 24 : 2096 - 103
- Aouacheria A , Cibiel A , Guillemin Y , Gillet G , Lalle P . 2007 ; Modulating mitochondria-mediated apoptotic cell death through targeting of Bcl-2 family proteins . Recent Pat DNA Gene Seq . 1 : 43 - 61
- Bellot G , Cartron PF , Er E , Oliver L , Juin P , Armstrong LC , Bornstein P , Mihara K , Manon S , Vallette FM . 2007 ; TOM22, a core component of the mitochondria outer membrane protein translocation pore, is a mitochondrial receptor for the proapoptotic protein Bax . Cell Death Differ . 14 : 785 - 94
- Billen LP , Kokoski CL , Lovell JF , Leber B , Andrews DW . 2008 ; Bcl-XL inhibits membrane permeabilization by competing with Bax . PLoS Biol . 6 : e147 -
- Borgne-Sanchez A , Dupont S , Langonne A , Baux L , Lecoeur H , Chauvier D , Lassalle M , Deas O , Briere JJ , Brabant M . 2007 ; Targeted Vpr-derived peptides reach mitochondria to induce apoptosis of alphaVbeta3-expressing endothelial cells . Cell Death Differ . 14 : 422 - 35
- Cartron PF , Arokium H , Oliver L , Meflah K , Manon S , Vallette FM . 2005 ; Distinct domains control the addressing and the insertion of Bax into mitochondria . J Biol Chem . 280 : 10587 - 98
- Chen Y , Xu X , Hong S , Chen J , Liu N , Underhill CB , Creswell K , Zhang L . 2001 ; RGD-Tachyplesin inhibits tumor growth . Cancer Res . 61 : 2434 - 8
- Dive C , Gregory CD , Phipps DJ , Evans DL , Milner AE , Wyllie AH . 1992 ; Analysis and discrimination of necrosis and apoptosis (programmed cell death) by multiparameter flow cytometry . Biochim Biophys Acta . 1133 : 275 - 85
- Ellerby HM , Arap W , Ellerby LM , Kain R , Andrusiak R , Rio GD , Krajewski S , Lombardo CR , Rao R , Ruoslahti E . 1999 ; Anti-cancer activity of targeted pro-apoptotic peptides . Nat Med . 5 : 1032 - 8
- Foillard S , Jin ZH , Garanger E , Boturyn D , Favrot MC , Coll JL , Dumy P . 2008 ; Synthesis and biological characterisation of targeted pro-apoptotic peptide . Chembiochem . 9 : 2326 - 32
- Foillard S , Sancey L , Coll JL , Boturyn D , Dumy P . 2009 ; Targeted delivery of activatable fluorescent pro-apoptotic peptide into live cells . Org Biomol Chem . 7 : 221 - 4
- Fuertes G , Giménez D , Esteban-Martin S , Garcia-Saez AJ , Sanchez O , Salgado J . Editor: Bioscience L . 2010 ; Role of Membrane Lipids for the Activity of Pore Forming Peptides and Proteins . Proteins: Membrane Binding and Pore Formation . Austin, TX Landes Bioscience ;
- Garcia-Saez AJ , Chiantia S , Salgado J , Schwille P . 2007 ; Pore formation by a Bax-derived peptide: effect on the line tension of the membrane probed by AFM . Biophys J . 93 : 103 - 12
- Garcia-Saez AJ , Coraiola M , Dalla Serra M , Mingarro I , Menestrina G , Salgado J . 2005 ; Peptides derived from apoptotic Bax and Bid reproduce the poration activity of the parent full-length proteins . Biophys J . 88 : 3976 - 90
- Garcia-Saez AJ , Coraiola M , Serra MD , Mingarro I , Muller P , Salgado J . 2006 ; Peptides corresponding to helices 5 and 6 of Bax can independently form large lipid pores . Febs J . 273 : 971 - 81
- Garcia-Saez AJ , Mingarro I , Perez-Paya E , Salgado J . 2004 ; Membrane-insertion fragments of Bcl-xL, Bax, and Bid . Biochemistry . 43 : 10930 - 43
- George NM , Evans JJ , Luo X . 2007 ; A three-helix homo-oligomerization domain containing BH3 and BH1 is responsible for the apoptotic activity of Bax . Genes Dev . 21 : 1937 - 48
- George NM , Targy N , Evans JJ , Zhang L , Luo X . Bax contains two functional mitochondrial targeting sequences and translocates to mitochondria in a conformational change- and homo-oligomerization-driven process . J Biol Chem . 285 : 1384 - 92
- Guillemin Y , Lopez J , Gimenez D , Fuertes G , Valero JG , Blum L , Gonzalo P , Salgado J , Girard-Egrot A , Aouacheria A . Active Fragments from Pro- and Antiapoptotic BCL-2 Proteins Have Distinct Membrane Behavior Reflecting Their Functional Divergence . PLoS One . 5 : e9066 -
- Heimlich G , McKinnon AD , Bernardo K , Brdiczka D , Reed JC , Kain R , Kronke M , Jurgensmeier JM . 2004 ; Bax-induced cytochrome c release from mitochondria depends on alpha-helices-5 and -6 . Biochem J . 378 : 247 - 55
- Jacotot E , Deniaud A , Borgne-Sanchez A , Touat Z , Briand JP , Le Bras M , Brenner C . 2006 ; Therapeutic peptides: Targeting the mitochondrion to modulate apoptosis . Biochim Biophys Acta . 1757 : 1312 - 23
- Jansson A , Sun XF . 2002 ; Bax expression decreases significantly from primary tumor to metastasis in colorectal cancer . J Clin Oncol . 20 : 811 - 6
- Jin ZH , Josserand V , Razkin J , Garanger E , Boturyn D , Favrot MC , Dumy P , Coll JL . 2006 ; Noninvasive optical imaging of ovarian metastases using Cy5-labeled RAFT-c(-RGDfK-)4 . Mol Imaging . 5 : 188 - 97
- Kjonniksen I , Storeng R , Pihl A , McLemore TL , Fodstad O . 1989 ; A human tumor lung metastasis model in athymic nude rats . Cancer Res . 49 : 5148 - 52
- Klepfish A , Greco MA , Karpatkin S . 1993 ; Thrombin stimulates melanoma tumor-cell binding to endothelial cells and subendothelial matrix . Int J Cancer . 53 : 978 - 82
- Kolluri SK , Zhu X , Zhou X , Lin B , Chen Y , Sun K , Tian X , Town J , Cao X , Lin F . 2008 ; A short Nur77-derived peptide converts Bcl-2 from a protector to a killer . Cancer Cell . 14 : 285 - 98
- Law B , Quinti L , Choi Y , Weissleder R , Tung CH . 2006 ; A mitochondrial targeted fusion peptide exhibits remarkable cytotoxicity . Mol Cancer Ther . 5 : 1944 - 9
- Lovell JF , Billen LP , Bindner S , Shamas-Din A , Fradin C , Leber B , Andrews DW . 2008 ; Membrane binding by tBid initiates an ordered series of events culminating in membrane permeabilization by Bax . Cell . 135 : 1074 - 84
- Ludtke SJ , He K , Heller WT , Harroun TA , Yang L , Huang HW . 1996 ; Membrane pores induced by magainin . Biochemistry . 35 : 13723 - 8
- Mader JS , Hoskin DW . 2006 ; Cationic antimicrobial peptides as novel cytotoxic agents for cancer treatment . Expert Opin Investig Drugs . 15 : 933 - 46
- Mai JC , Mi Z , Kim SH , Ng B , Robbins PD . 2001 ; A proapoptotic peptide for the treatment of solid tumors . Cancer Res . 61 : 7709 - 12
- Marks AJ , Cooper MS , Anderson RJ , Orchard KH , Hale G , North JM , Ganeshaguru K , Steele AJ , Mehta AB , Lowdell MW . 2005 ; Selective apoptotic killing of malignant hemopoietic cells by antibody-targeted delivery of an amphipathic peptide . Cancer Res . 65 : 2373 - 7
- Marr AK , Gooderham WJ , Hancock RE . 2006 ; Antibacterial peptides for therapeutic use: obstacles and realistic outlook . Curr Opin Pharmacol . 6 : 468 - 72
- Olea N , Villalobos M , Ruiz de Almodovar JM , Pedraza V . 1992 ; MCF-7 breast cancer cells grown as multicellular spheroids in vitro: effect of 17 beta-estradiol . Int J Cancer . 50 : 112 - 7
- Oltersdorf T , Elmore SW , Shoemaker AR , Armstrong RC , Augeri DJ , Belli BA , Bruncko M , Deckwerth TL , Dinges J , Hajduk PJ . 2005 ; An inhibitor of Bcl-2 family proteins induces regression of solid tumours . Nature . 435 : 677 - 81
- Ouyang H , Furukawa T , Abe T , Kato Y , Horii A . 1998 ; The BAX gene, the promoter of apoptosis, is mutated in genetically unstable cancers of the colorectum, stomach, and endometrium . Clin Cancer Res . 4 : 1071 - 4
- Papo N , Seger D , Makovitzki A , Kalchenko V , Eshhar Z , Degani H , Shai Y . 2006 ; Inhibition of tumor growth and elimination of multiple metastases in human prostate and breast xenografts by systemic inoculation of a host defense-like lytic peptide . Cancer Res . 66 : 5371 - 8
- Papo N , Shai Y . 2005 ; Host defense peptides as new weapons in cancer treatment . Cell Mol Life Sci . 62 : 784 - 90
- Qian S , Wang W , Yang L , Huang HW . 2008 ; Structure of transmembrane pore induced by Bax-derived peptide: evidence for lipidic pores . Proc Natl Acad Sci U S A . 105 : 17379 - 83

- Rege K , Patel SJ , Megeed Z , Yarmush ML . 2007 ; Amphipathic peptide-based fusion peptides and immunoconjugates for the targeted ablation of prostate cancer cells . Cancer Res . 67 : 6368 - 75
- Sancey L , Ardisson V , Riou LM , Ahmadi M , Marti-Batlle D , Boturyn D , Dumy P , Fagret D , Ghezzi C , Vuillez JP . 2007 ; In vivo imaging of tumour angiogenesis in mice with the alpha(v)beta (3) integrin-targeted tracer (99m)Tc-RAFT-RGD . Eur J Nucl Med Mol Imaging . 34 : 2037 - 47
- Schinzel A , Kaufmann T , Schuler M , Martinalbo J , Grubb D , Borner C . 2004 ; Conformational control of Bax localization and apoptotic activity by Pro168 . J Cell Biol . 164 : 1021 - 32
- Shiraishi T , Nielsen PE . 2006 ; Enhanced delivery of cell-penetrating peptide-peptide nucleic acid conjugates by endosomal disruption . Nat Protoc . 1 : 633 - 6
- Suzuki M , Youle RJ , Tjandra N . 2000 ; Structure of Bax: coregulation of dimer formation and intracellular localization . Cell . 103 : 645 - 54
- Terrones O , Antonsson B , Yamaguchi H , Wang HG , Liu J , Lee RM , Herrmann A , Basanez G . 2004 ; Lipidic pore formation by the concerted action of proapoptotic BAX and tBID . J Biol Chem . 279 : 30081 - 91
- Valentijn AJ , Upton JP , Bates N , Gilmore AP . 2008 ; Bax targeting to mitochondria occurs via both tail anchor-dependent and -independent mechanisms . Cell Death Differ . 15 : 1243 - 54
- Yip KW , Reed JC . 2008 ; Bcl-2 family proteins and cancer . Oncogene . 27 : 6398 - 406
- Youle RJ , Strasser A . 2008 ; The BCL-2 protein family: opposing activities that mediate cell death . Nat Rev Mol Cell Biol . 9 : 47 - 59
- Zong WX , Lindsten T , Ross AJ , MacGregor GR , Thompson CB . 2001 ; BH3-only proteins that bind pro-survival Bcl-2 family members fail to induce apoptosis in the absence of Bax and Bak . Genes Dev . 15 : 1481 - 6

Figure 1

Ectopic overexpression of GFP-tagged Bax-α5/α6 fragments induces cell death

(A) Chimeric GFP proteins used in this study. GFP-tagged constructs encoding GFP alone, or fusions of GFP with full-length Bax, Bax-α1, Bax-α5, Bax-α6, Bax-α5α6, Bax-α5-α9 and Bax-α9 are represented. The α-helical topology of Bax in solution was retrieved from (Suzuki et al., 2000). Because the structure of the membrane-bound form of Bax is unknown, we designed peptide versions that extend a few residues beyond the α-helical regions determined for the structure in aqueous buffer. (B) Expression and analysis of the various GFP-tagged proteins in mammalian cells. Western Blot analyses on transiently transfected HT1080 cells (24h post-transfection). Proteins were separated by SDS-PAGE followed by immunoblot with anti-GFP antibody (upper panel). Asterisks indicate the various GFP fusions depicted in (A). The expected sizes are 27, 48, 29, 30.2, 33.2, 37.2, 29.7 and 28.6 kDa respectively. Analysis of caspase-3 activation (low panel, the cleaved 17kDa product indicates activated caspase-3) and PARP cleavage (middle panel, the generated 29kD PARP fragment is shown). Similar results were obtained using MEF-DKO (not shown). (C) FACS assays of Annexin V staining in HT1080 cells. Transfected cells were stained for phosphatidylserine exposure using Cy3-conjugated Annexin V and the percentage of apoptotic GFP-expressing cells was determined by FACS. Histograms represent the percentage of GFP-expressing cells binding Annexin V (upper panel). Assays were performed in triplicate (error bars correspond to standard deviations). GFP-$[KLAKLAK]_2$ transfection and staurosporine (STS) treatment were included for comparison. (D) Primary FACS histogram overlays showing Annexin-V staining of MEF and MEF-DKO cells expressing GFP or GFP-Bax-α 5 and respectively treated with staurosporine (STS) or left untreated.

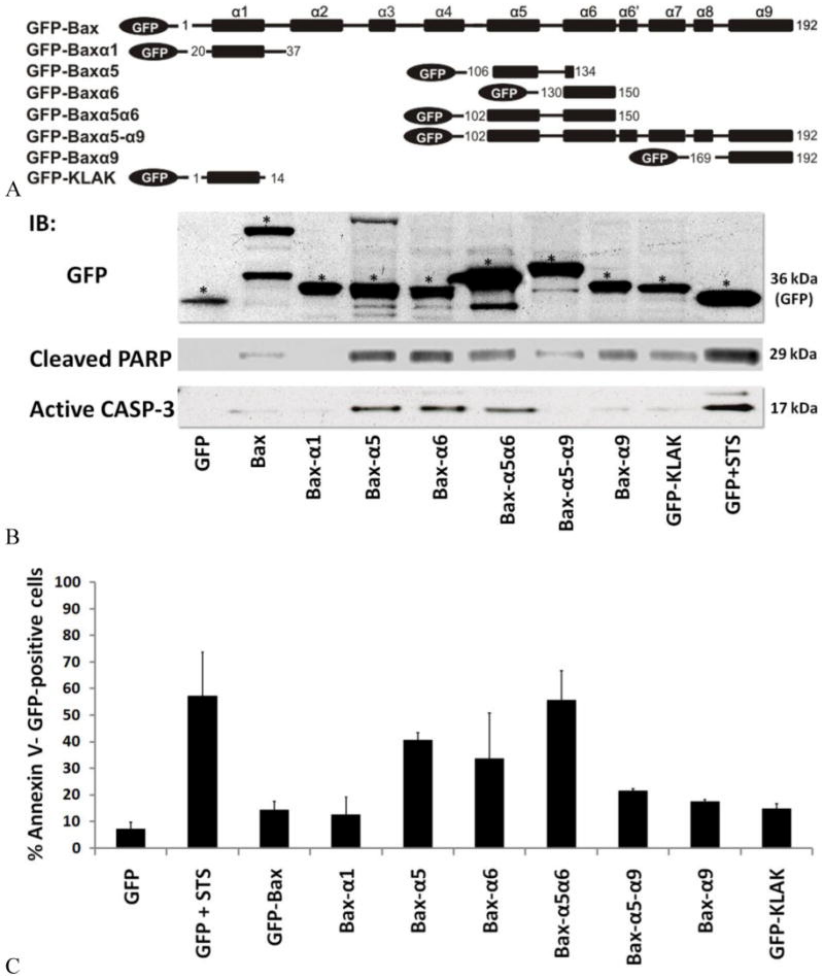

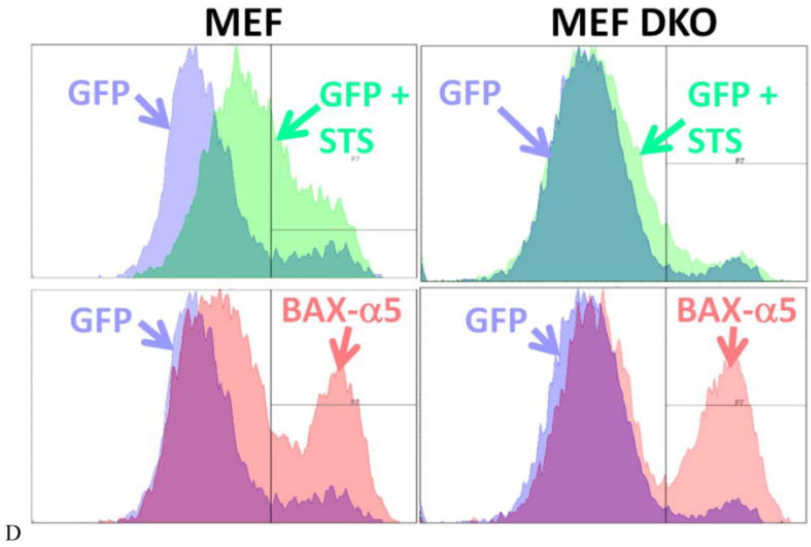

Figure 2

Subcellular localization of the GFP-tagged, Bax-derived (poly)peptides

MEF-DKO cells were co-transfected with mito-DsRed plasmid (encoding DsRed2 fused to the mitochondrial targeting sequence from subunit VIII of human cytochrome c oxidase) and the GFP-tagged constructs. Subcellular distribution was analyzed by confocal microscopy 24h after transfection. Confocal images showing GFP (green) and MitoDsRed (red) fluorescence. The DNA staining dye Topro-3 (blue) was used to visualize the nuclei. In merged images, the yellow color shows the co-localization of GFP and MitoDsRed in mitochondria. Similar images were obtained using an antibody detecting mitochondrial Hsp70 (low panel). Scale bar, 10 μm.

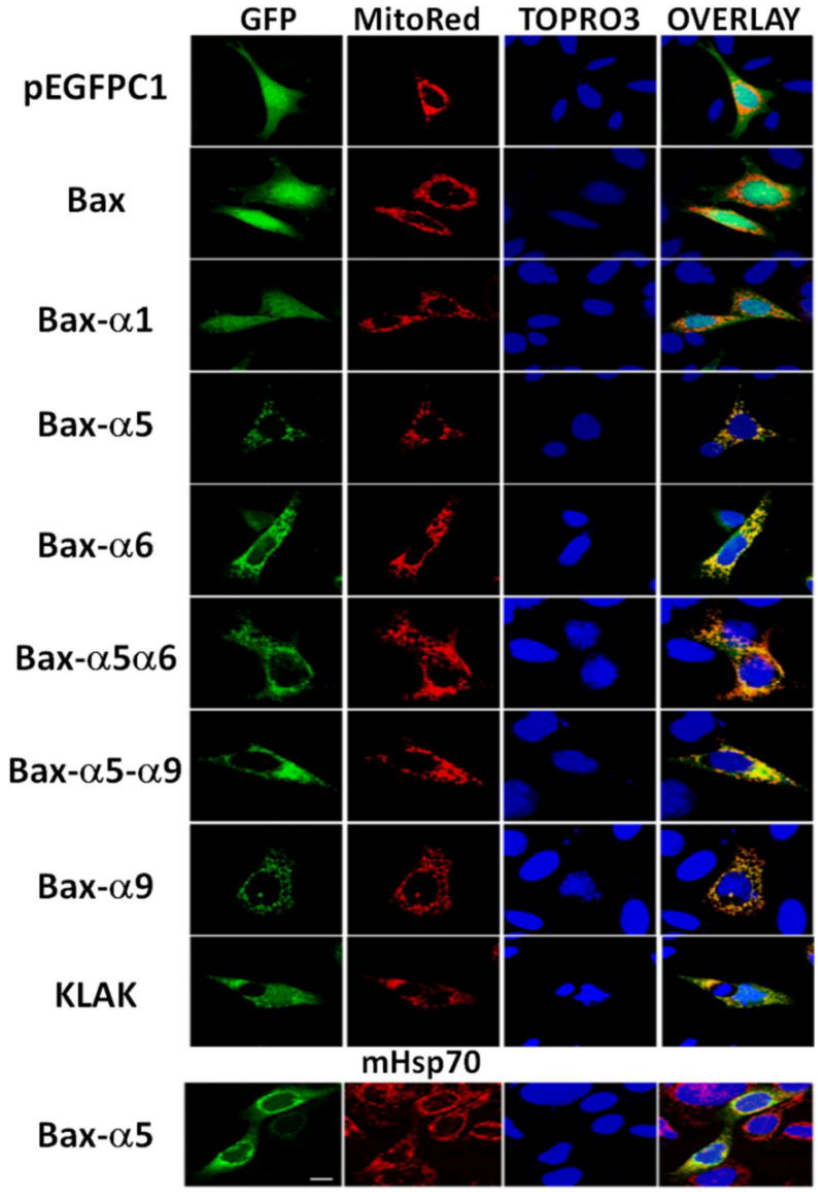

Figure 3

Effects of the GFP-tagged, Bax-derived (poly)peptides on mitochondrial membrane potential

ΔΨm was observed using the membrane potential sensitive probe Mitotracker-Red CMX-ROS. HT1080 cells were transfected with plasmids encoding the various GFP-tagged fusions and stained with Mitotracker-Red. GFP/Mitotracker-Red double-positive cells were counted (see Fig. S2 , top panel). Data were compiled from 3 different fields (40 × magnification). Data were compiled from 3 different fields (40 × magnification) and represented as mean values from three independent experiments, with error bars corresponding to ± SD. Similar results were obtained from three independent experiments. Analysis of ΔΨm changes by FACS gave similar results (Fig. S2 , middle and bottom panels).

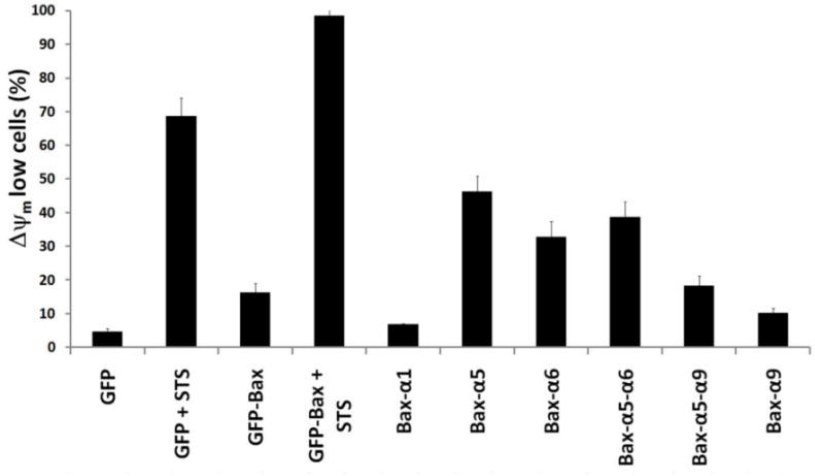

Figure 4

Synthetic peptide with the sequence of Bax[106-134] fused to an arginine octapeptide (R8-Bax[106-134]) is internalized into HeLa cells and induces caspase-dependent apoptosis

(A) HeLa cells were treated for 6h with 10 μM R8-Bax[106-134] or with a control peptide (R8-Bax[Scr]), both conjugated to fluorescein, and observed under phase-contrast (left) or FITC epifluorescence (right, green). Cells incubated with the R8(FITC)-conjugated peptides displayed intense cytoplasmic labelling (likely associated mainly with endosomes, as shown previously (Shiraishi and Nielsen, 2006)). Scale bar, 10 μ m. (B) Concentration- and time-dependent inhibition of cell viability of HeLa cells by R8-Bax[106-134]. HeLa cells were treated with various concentrations (5, 10, 25 and 50 μM) of R8-Bax[106-134] or R8-Bax[Scr] peptides. Cytotoxicity was assessed by measuring lactate dehydrogenase (LDH) release at 3, 6, 24h or 48h of incubation (n=4). R8-Bax[Scr] did not cause any significant LDH leakage for any of the concentrations tested. Data are represented as mean ± SD. (C) Caspase inhibitor zVAD.fmk reduced cell death in response to R8-Bax[106-134]. Cell death was assessed by measuring LDH leakage after 24h exposure to R8-Bax[106-134] (25 μM) in the absence (DMSO-treated cells) or presence of 100 μM zVAD.fmk. Data are represented as mean values ± SD. (D) Mode of cell death (apoptosis and necrosis) as revealed by Hoechst and propidium iodide double staining in HeLa cells treated with the R8-Bax[106-134] peptide. Cell death was quantified after 6h- or 24h treatment with 25 μM R8-Bax[106-134]. The mode of cell death, necrosis versus apoptosis, was determined by the cellular permeability to propidium iodide (necrosis) and the morphology of the nuclei after staining with Hoechst 33342 (apoptosis). Propidium iodide-negative cell with condensed or fragmented nuclei were counted as apoptotic. Data were compiled from 3 different fields (40 × magnification) and represented as mean values from three independent experiments ± SD.

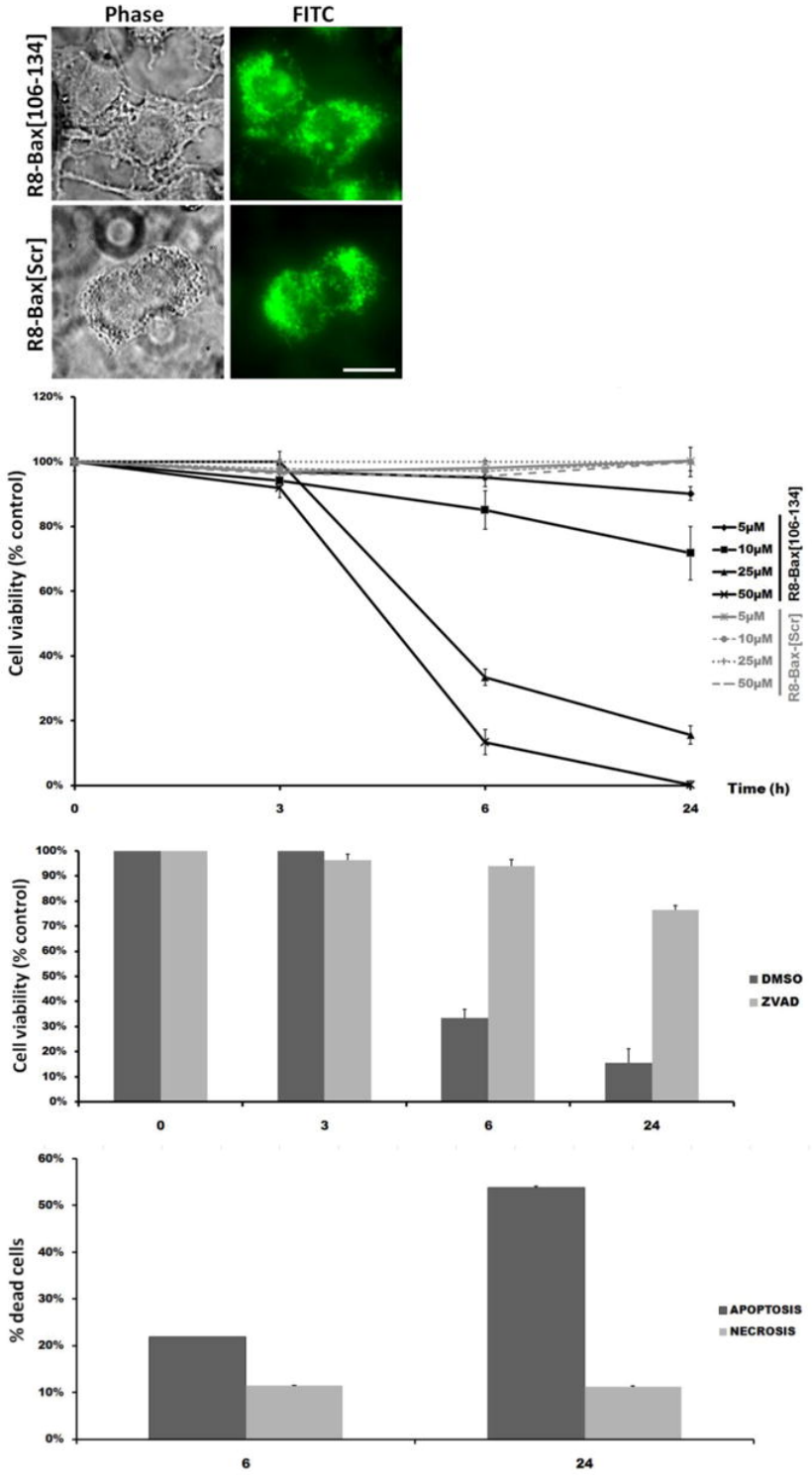
Phase
FITC
R8-Bax[106-134]
R8-Bax[Scr]
Cell viability (% control)
120%
100%
80%
60%
40%
20%
0%
0
3
6
24
Time (h)
5μM
10μM
25μM
50μM
R8-Bax[106-134]
R8-Bax[Scr]
Cell viability (% control)
DMSO
ZVAD
% dead cells
APOPTOSIS
NECROSIS

Figure 5

R8-Bax[106-134] induces Bax/Bak-independent, caspase-dependent apoptotic cell death

Effect of treatment of Bax/Bak-deficient mouse embryonic fibroblasts (MEF DKO) or wild-type fibroblasts (MEF) with either the FITC-conjugated peptide R8-Bax[106-134] or FITC-conjugated R8-Bax[Scr], in the absence or in the presence of zVAD.fmk (100μM). Apoptosis was measured by flow cytometry using Annexin V-Cy3 binding at 6h and 24h. Results are presented as the percentage of apoptotic cells that had internalized the FITC-conjugated peptide (Annexin V-Cy3+/FITC+) in each condition.

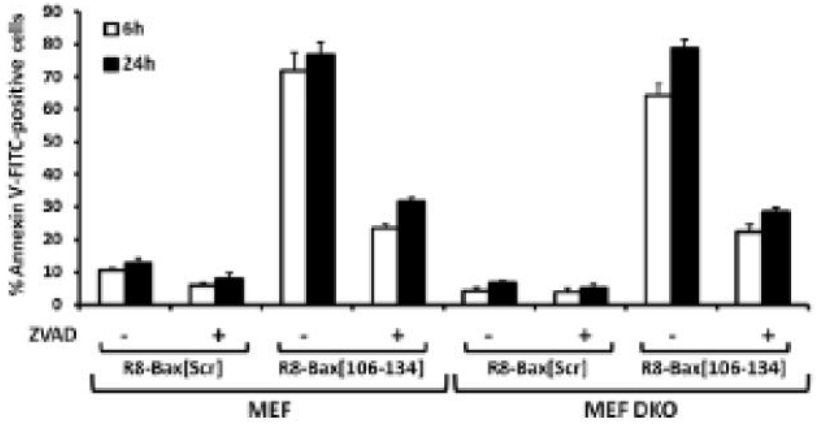

Figure 6

Antitumor effects induced by peritumoral injection of R8-Bax[106-134] in TS/A-pc mammary carcinoma xenografts

Mouse mammary TS/A-pc carcinoma growth inhibition by Bax[106-134]. Three days after injection of tumor cells, mice (9 mice/group) received vehicle (PBS), 100 μg of Bax[106-134], or 100 μg of Bax-Scr peritumorally, 5 times a week for 2 weeks (arrows). Tumor volumes are indicated as mean values ± S.E.M. The tumor doubling times (Days ± S.E.M) were 0.493 ± 0.034 for the control group (*P vs* . Scramble = 0.7963, not significant), 0.692 ± 0.055 for the R8-Bax[106-134] group (*P vs* . control = 0.0072 **/*P vs* . Scramble = 0.0063 **) and 0.480 ± 0.039 for the R8-Bax[Scr] group (*P vs* . control = 0.7963, not significant). *Inset* : protein levels of active caspase-3 in tumor extracts from each group were determined by immunoblotting. To ensure equal protein loading, membranes were also probed for tubulin. Data from triplicate samples are shown.